IOP Publishing Journal of Geophysics and Engineering
J. Geophys. Eng. **8** (2011) 46–60 doi:10.1088/1742-2132/8/1/007

Ground-motion predictive equations for low-magnitude earthquakes in the Campania–Lucania area, Southern Italy

A Emolo[1,3], V Convertito[2] and L Cantore[1]

[1] Dipartimento di Scienze Fisiche, Università degli Studi 'Federico II', Napoli, Italy
[2] Istituto Nazionale di Geofisica e Vulcanologia, Osservatorio Vesuviano, Napoli, Italy

E-mail: antonio.emolo@unina.it

Received 1 June 2010
Accepted for publication 1 November 2010
Published 9 December 2010
Online at stacks.iop.org/JGE/8/46

Abstract
A key aspect of ground-shaking map calculation is represented by ground-motion predictive equations (GMPEs). In fact, ground-shaking maps obtained soon after an earthquake are calculated by integrating observed data and ground-motion estimates from GMPEs for those areas not covered by seismic stations. Empirical ground-motion models that are used to obtain these estimates refer primarily to strong ground-motion due to large earthquakes and cannot be properly used to estimate the effects of small magnitude seismic events. In this paper we calibrated GMPEs for low-magnitude earthquakes from data recorded at the seismographic stations of the Irpinia Seismic Network, in the Campania–Lucania region, Southern Italy. In particular, the available dataset is formed by peak ground acceleration (PGA) and velocity (PGV) parameters coming from 123 earthquakes (local magnitudes ranging between 1.5 and 3.2) recorded at 21 stations of the ISNet network at hypocentral distances from 3 km to about 100 km. The total number of peaks measurements is 875. This study is part of a research project, in collaboration with the Italian Department of Civil Protection and National Institute of Geophysics and Volcanology, aimed at producing ground-motion shaking maps.

Keywords: ground-motion predictive equations, ground-shaking map, seismic hazard

1. Introduction

Implementation of codes aimed at calculating ground-shaking maps, in the last few years, has increasingly attracted a large number of regions worldwide and Italy as well (e.g., Michelini *et al* 2008, Convertito *et al* 2010, Iannaccone *et al* 2010). Ground-motion shaking maps are calculated by integrating real data recorded at stations belonging to a given seismic network and predictive estimates for those areas not covered by the network (Wald *et al* 1999, Convertito *et al* 2010). The technique used to obtain ground-motion estimates at sites not covered by seismic network depends on the time-scale of interest. When near-real time is of interest, for example for Civil Protection purposes, estimates are obtained from ground-motion predictive equations (hereinafter, GMPEs).

The GMPEs are empirical equations that provide strong ground-motion parameters, given the earthquake magnitude and the source-to-site distance. As a consequence, the reliability of the ground-motion shaking maps depends on the selected GMPE and on the available dataset used to retrieve its coefficients: the more representative the dataset is (e.g., in terms of magnitude values, source-to-site distances, site conditions, and so on) the more reliable the estimates will be. In this respect, a further aspect to account could be the fact that estimates obtained by using the GMPE models retrieved on a given dataset collected in a particular tectonic area should not be used in a different tectonic area. This is particularly important for low-magnitude earthquakes for which attenuation effects, related to the tectonic area of interest, can be predominant with respect to the source effects (Douglas 2007).

[3] Author to whom any correspondence should be addressed.

Additionally, GMPEs play an important role both in seismic hazard analysis and in the earthquake early-warning applications. In both cases, even if within different time-scales, estimates of the effect of the occurrence of earthquakes in a given magnitude range are required. Those estimates correspond, for example, to peak ground-motion parameters and associated probability density functions.

Nowadays, empirical ground-motion models used to compute ground-shaking maps or to perform seismic hazard analyses refer to strong ground-motion produced by moderate-to-large earthquakes. Just to cite some examples, Abrahamson and Silva (1997) used a database starting at magnitude 4.4, Akkar and Bommer (2007) have a lower magnitude limit of 5.5, and Boore and Atkinson (2008) have a lower limit of 5.0. As a consequence, they cannot be properly used to predict ground-motion associated with low-magnitude earthquakes. On the other hand, frequent, shallow low-magnitude earthquakes have an important influence in seismic hazard analysis, particularly at intermediate and long return periods for which the effect of a large frequency of occurrence may be more important than the effect of the occurrence of a single large earthquake (Reiter 1990). Those considerations entail the importance of retrieving and/or refining the GMPEs for low-magnitude seismic events.

The motivation of this paper relies on the collaboration with the Italian Department of Civil Protection (DPC) and National Institute of Geophysics and Volcanology (INGV) in the framework of the research project S3 of agreement 2007–2009 between DPC and INGV. This project aims at providing tools for computing ground-shaking maps for the whole Italian peninsula, thus requiring regional GMPEs for both low and moderate-to-large earthquakes.

Following the analogous studies performed by Frisenda *et al* (2005) for the Lunigiana–Garfagnana region (Central Italy) and Massa *et al* (2007) for Central-Northern Italy, the aim of this paper is the estimation of a GMPE for low-magnitude earthquakes in the Campania–Lucania region, in Southern Italy, to be used for ground-shaking map calculation. In particular, our modelling concerned the peak ground acceleration (PGA) and velocity (PGV) and, due to their use in the ground-shaking map framework, the results will refer to rock-site conditions.

A two-step procedure has been applied to retrieve the best GMPE. First of all, the available data, consisting of PGAs and PGVs measured from waveforms corresponding to 123 earthquakes recorded in the area of interest, are arranged in bins, both with respect to the magnitude and to the distance. PGAs and PGVs are then reduced to rock-site conditions following the same procedure implemented in the codes used for ground-shaking map computation. In practice, these codes use corrective coefficients for peak parameters, based on geological maps obtained by grouping the main geological formation outcropping in the area of interest (Wald *et al* 1999, Convertito *et al* 2010). With the same aim, we adopted the geological macro-zoning of the Campania–Lucania region (Southern Italy) obtained by Cantore (2008) and Cantore *et al* (2010) who grouped the main geological units according to the Quaternary-Volcanic-Tertiary-Mesozoic (QVTM) classification, and also assigned a site-specific coefficient to each class. These coefficients have been used for correcting the peak ground-motion quantities. The available PGAs and PGVs, reduced in this way to rock site, are then used to retrieve a reference GMPE.

In the next step, we computed, for each site in which data are available, the residual distribution between observed and predicted ground-motion parameters, the latter obtained by using the reference GMPE. Then, we performed a *Z*-test, with a 5% significance level, in order to discriminate those sites characterized by the residual distribution having a mean significantly different from zero, thus indicating a station effect that cannot be exhaustively accounted for by using the corrective coefficients. Based on the *Z*-test results, we associated a dummy variable s with each site, whose value is 1 if the mean residual value is significantly different from zero and positive, -1 if the mean is significantly different from zero and negative, 0 otherwise. Station-effect can play an important role in the ground-shaking map calculation. This is the case, for example, of the ShakeMap® code that uses a corrective coefficient, named *bias*, which is based on the residuals between observed and estimated data. The *bias* correction aims at reducing errors related, for instance, to the magnitude and location of the specific earthquake under study (Wald *et al* 1999).

The GMPEs obtained in this study have been finally compared with the two models for low-magnitude earthquakes available for Italian regions, specifically the Frisenda *et al* (2005) and the Massa *et al* (2007) models, even if they have been retrieved in tectonic contexts different form the area we have analysed. The results of the comparison have shown that, at least for the low-magnitude earthquakes considered in this study, the tectonic regime can influence the peak ground-motion attenuation.

2. Dataset description and data processing

The data used in this paper have been collected by the stations belonging to the Irpinia Seismic Network (ISNet) in the last 5 years, starting from the network activation in September 2005. ISNet is a high dynamic-range, dense, seismographic network that has been deployed in Southern Italy, along the Campania–Lucania Apennines (Weber *et al* 2007, Iannaccone *et al* 2010), where large historical earthquakes occurred in the past (figure 1(*a*)). The network covers an area of about 100 km × 70 km (figure 1(*b*)), with the aim of monitoring the active seismic faults system that generated the last destructive 1980, M_S6.9, Irpinia earthquake (Bernard and Zollo 1989). ISNet has also been designed to be the backbone infrastructure for a regional earthquake early-warning system (EEWS, e.g., Allen and Kanamori 2003) that, at present, is under development (Iannaccone *et al* 2010).

ISNet network is currently composed of 29 seismic stations and five local control centers that act as data storage and processing sites. All of the stations (black triangles in figure 1(*b*)) are equipped with a three-component accelerometer (Güralp CMG-5T) and a three-component velocimeter (Geotech S-13J) having a natural period of 1 s, thus ensuring a high-dynamic recording range. Five stations

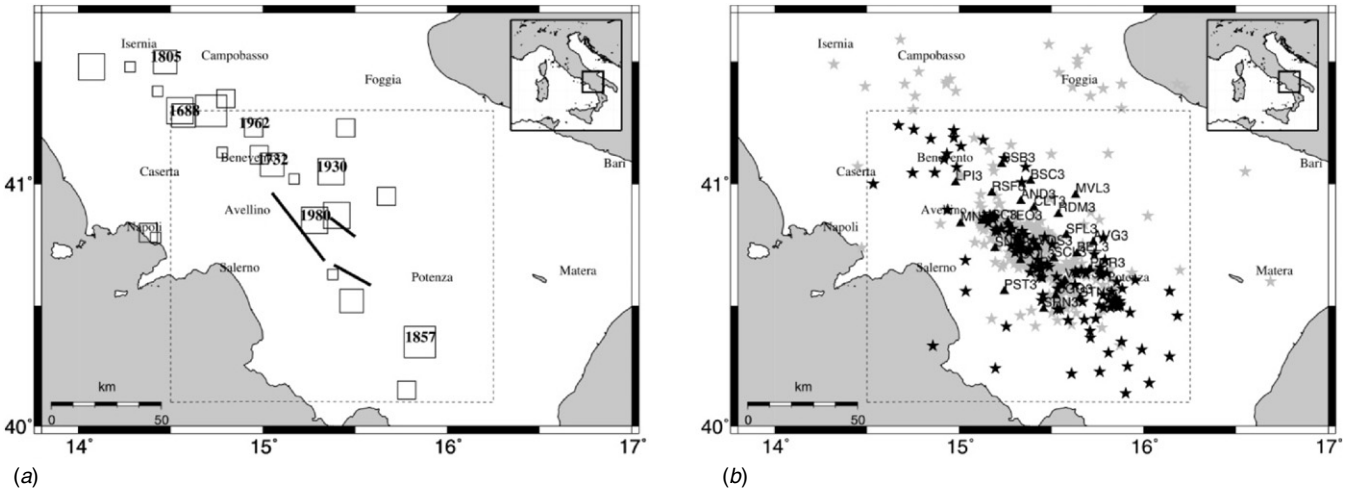

Figure 1. (*a*) Main historical earthquakes occurred in the area of interest for this study, retrieved from Boschi *et al* (1995). The last large event in the area occurred on 23 November 1980 (M_S6.9). This event, that is the strongest instrumental earthquake recorded in Italy, activated three different normal-fault segments in a time-span of about 40 s (Bernard and Zollo 1989). The traces of the faults that produced the 1980 earthquake are indicated as black thick lines. (*b*) The stars represent the whole recent seismicity recorded by the Irpinia Seismic Network (ISNet). In particular, black stars correspond to the epicenters of the earthquakes analysed in this study. The triangles are the seismographic stations of the ISNet network, each of which is identified by a four-letter station code. In both panels, the dashed lines define the 120 × 120 km^2 area of interest.

feature a broad-band velocimeter (Nanometrics Trillium, 0.025–50 Hz) to record both regional and teleseismic events. Concerning the accelerometers, the full recording dynamic range is set at ±1 *g* (*g* being the gravity acceleration) and their sensitivity is sufficient to record M1.5–2.0 events also at hypocentral distances larger than 40 km. The data-loggers are the Osiris-6 produced by Agecodagis Sarl.

The recent seismicity recorded at ISNet stations is represented as stars in figure 1(*b*). The largest part of the seismicity is located along the Apenninic belt chain and around the area containing the seismogenic structure responsible for the 23 November 1980, M_S6.9 earthquake, that was the last large earthquake in the area. The 1980 earthquake was generated by the activation of three distinct normal-fault segments in a very short time span. The traces of these three segments are represented in figure 1(*a*) as black thick lines.

For building our database, we excluded both seismic events located outside the area of interest (enclosed by the dashed lines in figure 1) and earthquakes characterized by a local magnitude lower than 1.5. Ultimately, we have selected, for this study, 123 earthquakes whose epicenters are identified as black stars in figure 1(*b*).

Some automatic procedures implemented at the Network Control Center in Naples are able to identify a seismic event at the ISNet stations and to localize it (Iannaccone *et al* 2010). In any case, all the events are then manually re-localized and a local magnitude value M_L is assigned to them according to the magnitude scale calibrated for Southern Italy and proposed by Bobbio *et al* (2009). Moreover, hypocentral coordinates and local magnitude provided by INGV are assigned to those earthquakes whose location is external to the network. Bobbio *et al* (2009) demonstrated, in any case, that their local magnitude scale and the INGV local magnitude scale do not differ substantially and then they can be used in the same dataset without introducing any bias related to different formulations.

The dataset used for retrieving the GMPEs for the area of interest is formed by peak values (PGAs and PGVs) measured from seismograms corresponding to selected earthquakes. We defined the peak ground-motion acceleration as the larger value between the two horizontal components of the accelerograms recorded by CMG-40T sensors. It should be noted that some authors (e.g., Beyer and Bommer 2006) measure the peak value from the geometric mean of the horizontal components of ground-motion, in order to account for possible sensor mis-orientation that could affect the measure. Preliminary analyses have shown that, for the dataset used in this study, our definition of peak ground-motion does not significantly differ from that based on the geometrical mean.

Preliminarily, all the records have been processed applying a de-trending and band-pass filtering, in the range 0.075–20 Hz, by a four-pole Butterworth filter. PGA values are measured from acceleration records having a signal-to-noise ratio greater than 5 and within a time window which includes 5% to 95% of the total energy (Trifunac and Brady 1975). Figure 2 shows the scatter plot for the PGA dataset used to calibrate the ground-motion predictive equation. The local magnitude of the 123 selected earthquakes ranges between 1.5 and 3.2, while the hypocentral distance is in the range 3–100 km. The total number of available acceleration peaks is 875. Note that, despite the relatively short period of activity of ISNet, there is quite a uniform coverage with respect to the selected magnitude and hypocentral distance ranges.

The procedure for measuring PGVs is just a little different. In fact, the accelerograms used for obtaining the PGAs are integrated in the time domain and band-pass filtered in the

Table 1. Site class definitions for the Campania–Lucania region and the corresponding Eurocode 8 (EC8) from CEN, European Committee for Standardization (2004). After Cantore (2008).

Ground type	Age	$V_{S,30}$ (m s^{-1})	EC8 class
Carbonate platform succession	Mesozoic	> 800	A
Sediments, soft rocks and flysh deposit	Tertiary	360–800	B
Volcanic rocks	Quaternary-Tertiary	360–1000	B
Alluvium and gravel deposits	Quaternary	180–360	C
Very soft soils	Quaternary	<180	D

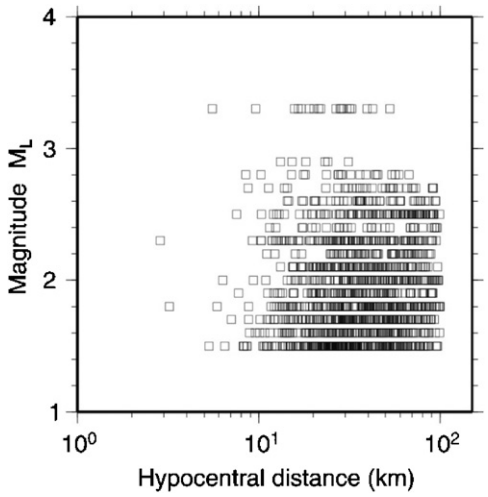

Figure 2. Scatter plot of the PGA values, available for this study, as a function of the magnitude and hypocentral distance. The scatter plot for PGV is completely equivalent.

frequency range 0.5–25 Hz before performing the measure. We did not use the peak values obtained directly from velocity records because the dataset is not homogeneous in time because the velocimeters installation and calibration is more recent than the accelerometers. The scatter plot for PGV is completely analogous to that for PGA shown in figure 2.

As an example, we report in table A1 in the appendix some PGA and PGV values, relating to some selected earthquakes, that are representative of the whole available database.

3. Geological macrozonation of the Campania–Lucania region

In order to retrieve a GMPE to be used for ground-shaking map calculation, all the data have to be first reduced to rock site. The procedure used in this study to that aim is completely equivalent to that proposed by Wald *et al* (1999). In particular, local site amplification effects on ground-shaking maps are accounted for by using empirical corrective coefficients whose values depend on both the soil lithology and the amplitude and frequency content of the input ground-motion. The amplification effects of near-surface geological layers critically depend on the shear-wave velocity and the thickness of the layers (e.g., Borcherdt 1970, 1994, Joyner and Fumal 1985).

In this paper we use the classification proposed by Cantore (2008) and Cantore *et al* (2010). Following the approach proposed by Park and Elrick (1998), the classification was

Table 2. Corrective coefficients for three frequency bands and for Mesozoic (M) and Tertiary (T) soils. After Cantore *et al* (2010).

Frequency band (Hz)	1–5	5–10	10–20
Coefficient for T soil	1.605	1.550	1.095
Coefficient for M soil	1.385	1.562	1.217

obtained by grouping the main geological units present in the area of interest into four macro-classes described by units having similar ages. Those macro-classes are considered representative of alluvium (Quaternary, Q), volcanic rock (Tertiary-Volcanic, T-V), soft rock (Tertiary, T) and hard-rock (Mesozoic, M). The four classes have been overlapped on the 1:250 000 scale regional map tracing only the geologic contacts separating units belonging to different categories. Then, based on a set of available geotechnical soundings, borehole measurements and surface geology, a range of shear-wave velocities for the near-surface layer ($V_{S,30}$) were assigned to each defined class.

Table 1 lists the $V_{S,30}$ associated with each of the geological units classified following the main indications proposed by Eurocode 8 (CEN, European Committee for Standardization 2004).

The map reporting this classification for the Campania–Lucania region is indicated as a 'QVTM map' and is shown in figure 3. Table 2 lists the corrective coefficients obtained by Cantore (2008) and Cantore *et al* (2010) for the PGA and PGV estimates at a rock site for the two main geology classes of interest in this study, i.e. M and T classes.

4. Ground-motion predictive equations for PGA and PGV

GMPEs have been retrieved by using a two-step procedure which aims first at finding the best model for the rock-site condition, and then at discriminating the stations which present deviations with respect to this model, thus indicating the presence of a station effect. Station effect accounts for all those effects that cannot be taken accurately into account by the corrective coefficients corresponding to the QVTM map, such as topography or specific site effects related to the first layers below the station and also not accounted for by the GMPE model.

As mentioned above, in this study we used PGA and PGV data from ground acceleration recorded at 21 stations belonging to the ISNet network. It should be noted that some stations that are present in the actual ISNet configuration have been recently installed and are still under calibration. For this

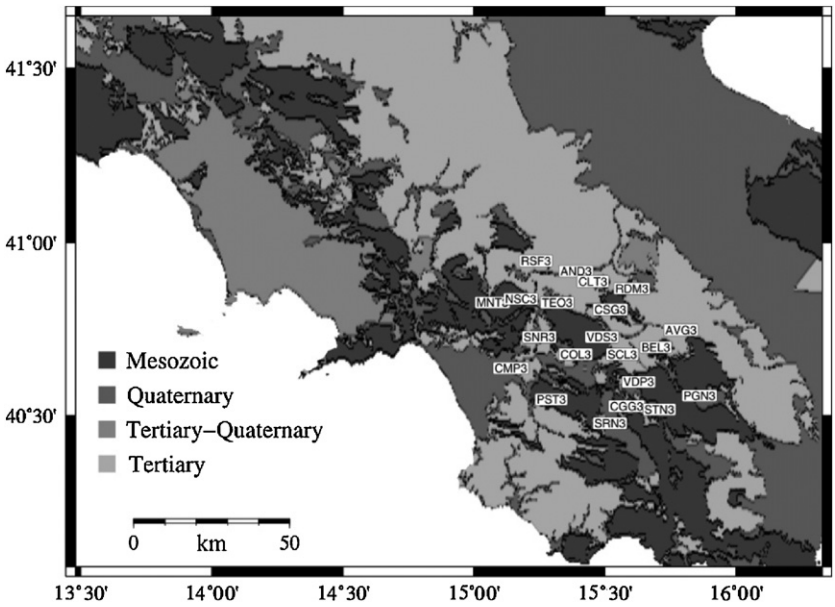

Figure 3. The QVTM classification map. The legend reports the correspondence between colors and geology. The labels indicate the locations of the ISNet seismic stations. After Cantore (2008).

reason, we limited our analyses to data coming from only 21 stations.

In the first step, the QVTM map shown in figure 3 is used to identify the site class on which each station is located. The stations of the ISNet network that have been considered in this study are predominantly located on two geological classes: thirteen stations are placed on Mesozioc soil while eight stations are on Tertiary soil. The corrective coefficients provided by Cantore (2008) and Cantore *et al* (2010) for these two soil classes are given in table 2 as a function of the frequency. These coefficients are used to reduce both PGAs and PGVs to rock-site condition.

In particular, for both the geological classes, PGA values were corrected by using the coefficients relative to the 10–20 Hz frequency band while the coefficients relating to the 5–10 Hz frequency band were used to correct PGVs. The frequency bands we selected for correcting the peak values correspond to the frequency ranges where the horizontal-to-vertical spectral ratios, computed on the S-waves window from earthquake waveforms recorded at ISNet stations, show amplification significantly different from unity (Cantore 2008).

The data reduced to rock site as described above have been used to retrieve a reference GMPE. The station effect has been then identified analysing the distributions of residuals with respect to the reference model for each station. Once the residuals distributions were available, we performed a *Z*-test at a 5% significance level to test the null-hypothesis 'mean value of residuals equal to zero'. In this way, it is possible to assign a dummy variable *s* to each station, whose value depends on the result of the test and on the mean value of residuals. Finally, a new GMPE characterized by this additional parameter is retrieved.

4.1. Reference ground-motion model

We start selecting for the GMPEs the classical formulation given by

$$f(Y) = a + f_1(M) + f_2(R), \tag{1}$$

where Y is the ground-motion parameter to be predicted, $f_1(M)$ is a function of the magnitude and $f_2(R)$ is a function of the distance. In particular, in this study we assume that PGAs and PGVs are expressed in m s^{-2} and m s^{-1}, respectively. Moreover, M represents the local magnitude while R is the hypocentral distance in km.

Because the distribution of Y values is well approximated by a log-normal distribution (Reiter 1990), we set in equation (1) $f(Y) = \log Y$.

We tested different functional forms for the functions $f_1(M)$ and $f_2(R)$ in equation (1). The function $f_1(M)$, depending on the magnitude, was initially formulated according to the model used by Bragato and Slejko (2005) and Frisenda *et al* (2005) given by

$$f_1(M) = bM + b'M^2. \tag{2}$$

This equation accounts for the expected increasing of Y with the increasing of magnitude but, differently from many other models, contains a quadratic term that is introduced by some authors (e.g., Akkar and Bommer 2007) that dominates at large magnitude values. After some preliminary analyses performed on our dataset, we found that the coefficient b' in equation (2) was not statistically different from zero. As a consequence, we removed the quadratic term from the function $f_1(M)$, keeping only the linear dependence on the magnitude.

To investigate the attenuation due to geometrical spreading and the anelastic attenuation, the $f_2(R)$ function was first formulated as

$$f_2(R) = c \log R + c'R, \tag{3}$$

Table 3. Regression coefficients and associated standard errors for the reference ground-motion predictive equations for PGA and PGV whose general formulation is given by equation (4).

Y	a	b	c	$\sigma_{\log Y}$
PGA (m s^{-2})	−2.024	0.469	−1.442	0.444
PGV (m s^{-1})	−3.943	0.540	−1.458	0.359

where the two terms account for the geometrical and anelastic attenuation, respectively. Our preliminary analyses on the available dataset provided a value for the c' coefficient very close to zero. This means that peak ground-motion values are mainly affected by the geometrical spreading rather than by the anelastic attenuation. As a consequence, we removed the term related to anelastic attenuation from equation (3).

To summarize, the model we used for performing the regression analysis of the available dataset aimed at retrieving the reference GMPEs is given by

$$\log Y = a + bM + c\log(R) \pm \sigma_{\log Y}, \quad (4)$$

where Y corresponds either to PGA (measured in m s^{-2}) or to PGV (measured in m s^{-1}), M is the local magnitude, R is the hypocentral distance (expressed in km) and $\sigma_{\log Y}$ is the standard error associated with the random variable $\log Y$.

The coefficients inferred for the reference GMPEs along with the standard deviations are provided in table 3.

4.2. Residuals analysis and station corrections

As said before, in order to identify possible station effects which cannot be adequately taken into account by the corrective coefficients associated with the QVTM map, we analysed the residuals, for both PGA and PGV, with respect to the reference GMPEs. We define the residuals (RES) as

$$\mathrm{RES} = \ln Y^{\mathrm{obs}} - \ln Y^{\mathrm{pred}}, \quad (5)$$

where Y^{obs} and Y^{pred} represent the observed and predicted peak ground-motion values, respectively, the predicted values being estimated through the reference GMPE (equation (4)) with the appropriate coefficient given in table 3.

The residuals distributions at each station are shown in figures 4 and 5 for PGA and PGV, respectively. It is worthwhile to note that the offset of the residuals distribution is small compared with the dispersion of the overall distribution suggesting that, although a station effect was present, its contribution to the total sigma is modest, in agreement with the findings of Atkinson (2006).

In order to quantify the presence or not of station effects, we performed a Z-test, at 5% significance level, to test the null hypothesis of zero mean distribution. The stations LIO3 and SFL3 were excluded from the test because of their limited number of available data (less than 30). Concerning PGA, the residuals analysis allowed us to identify the stations CGG3, CMP3, COL3, PST3, RSF3, TE03 and VDP3 as not affected by a relevant station effect. On the other hand, when the PGV parameter is considered, all the stations seem to be affected by the station effect.

We introduced, in the predictive equation model, a dummy variable named s, which assumes a value of −1, 0 or 1

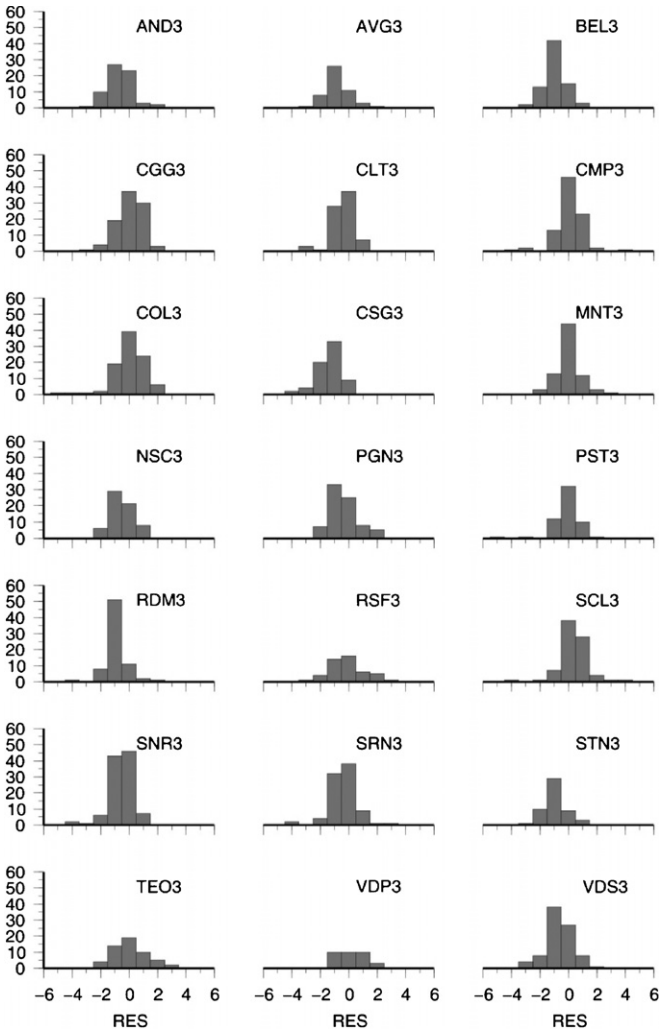

Figure 4. Residuals distributions for PGA at each station of the ISNet network. Residuals are defined according to equation (5) and are computed against the predictions obtained through the reference GMPEs (equation (4)) with the appropriate coefficients provided in table 3.

according to the sign of the mean residuals (significantly negative, zero, or significantly positive, respectively). Table 4 summarizes the results from the residuals analysis for all the stations for both PGA and PGV. The table also lists the calculated z-values which have been compared with the critical value $z_c = \pm 1.96$.

4.3. Corrected ground-motion model

Once each station has been classified according to the procedure described above, it is possible to consider a station-dependent model adding an additional term to the model given in equation (4) which becomes

$$\log Y = a + bM + c\log(R) + \mathrm{d}s \pm \sigma_{\log Y}, \quad (6)$$

where s is the dummy variable that characterizes the receiver (see table 4) and assumes values −1, 0 or 1.

The coefficients of equation (6), retrieved through regression analysis of ground-motion peaks, along with the standard error are given in table 5. Comparing the new

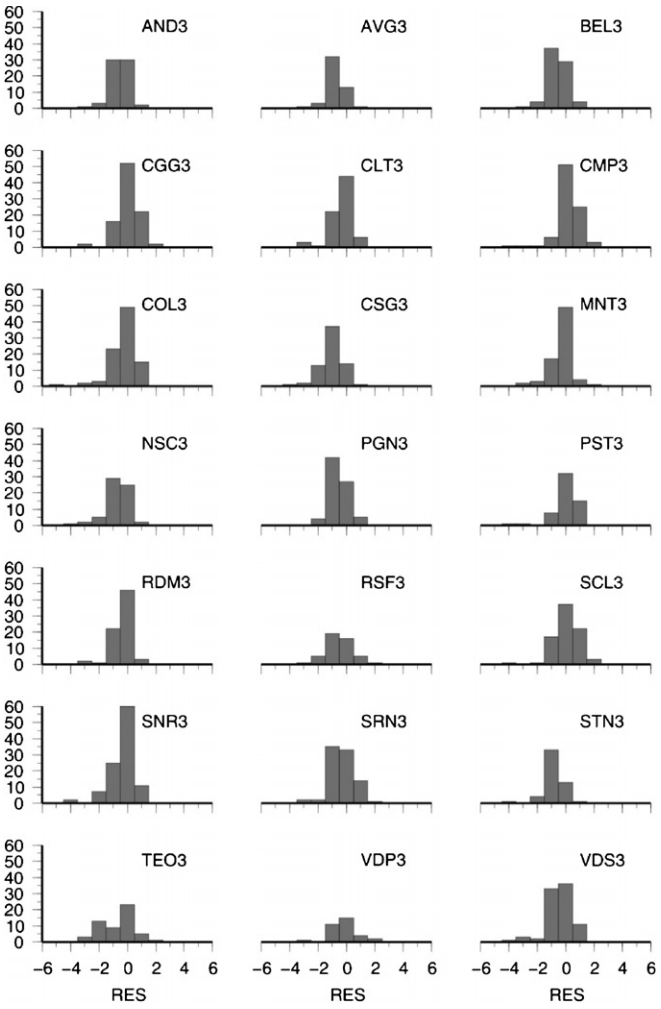

Figure 5. Same as figure 4 but for PGV.

coefficients with respect to those obtained for the reference model (table 3), it can be noted that the addition of the term d significantly affects only the a coefficient and, moreover, reduces the standard error σ, both for PGA and PGV. In both cases, we have verified, applying the Akaike Information Criterion (Emolo and Zollo 2005), that the reduction in the standard error is significant.

In order to check the reliability of our corrected GMPEs (equation (6) with coefficients given in table 5), we compared them with respect to the models proposed by Frisenda *et al* (2005) (hereinafter, FRI05) and Massa *et al* (2007) (hereinafter, MAS07) retrieved by using peak data from small earthquakes (magnitude less than 5.1 for FRI05 and 5.2 for MAS07) recorded in Central and Central-Northern Italy, respectively.

The MAS07 model has the same formulation as our GMPE (equation (6)), aside from a site-effect term that fairly corresponds to the station-effect s introduced in this study. Differently, the FRI05 model contains a quadratic dependence on the magnitude (as in equation (2)) that was introduced by the authors to assign a larger weight to the larger-magnitude earthquakes.

Table 4. For each station of the ISNet network the QVTM class is reported (M stands for Mesozoic soil and T for Tertiary soil) after Cantore *et al* (2010). For both PGA and PGV, the value of the statistical variable z used to perform the Z-test of hypothesis of the residuals is reported. The dummy variable s has been assigned to each station, for PGA and PGV, as a consequence of the hypothesis test results.

		PGA		PGV	
Station code	QVTM	z-value	s	z-value	s
AND3	T	−0.68	−1	−0.63	−1
AVG3	T	−0.79	−1	−0.84	−1
BEL3	T	−0.95	−1	−0.60	−1
CGG3	M	−0.02	0	0.05	1
CLT3	T	−0.46	−1	−0.36	−1
CMP3	M	0.33	0	0.19	1
COL3	M	0.00	0	−0.26	−1
CSG3	M	−1.42	−1	−1.03	−1
MNT3	M	−0.04	−1	−0.34	−1
NSC3	M	−0.48	−1	−0.65	−1
PGN3	M	−0.40	−1	−0.57	−1
PST3	M	−0.15	0	−0.02	−1
RDM3	T	−0.86	−1	−0.43	−1
RSF3	T	−0.11	0	−0.54	−1
SCL3	M	0.34	1	0.05	1
SNR3	M	−0.60	−1	−0.34	−1
SRN3	M	−0.37	−1	−0.29	−1
STN3	M	−0.37	−1	−1.03	−1
TEO3	T	0.04	0	−0.63	−1
VDP3	T	0.29	0	−0.26	−1
VDS3	M	−0.63	−1	−0.46	−1

Table 5. Regression coefficients and associated standard errors for the corrected ground-motion predictive equations for PGA and PGV whose general formulation is given in equation (6).

Y	a	b	c	d	$\sigma_{\log Y}$
PGA (m s^{-2})	−1.817	0.460	−1.428	0.271	0.417
PGV (m s^{-1})	−3.673	0.543	−1.463	0.120	0.347

The comparison has been performed classifying all the available data in three local-magnitude classes: M_L^1 (1.5, 2.0), M_L^2 (2.0, 2.5), and M_L^3 (2.5, 3.0). Due to the ISNet completeness threshold, we discarded all the seismic events having a magnitude lower than 1.5. Moreover, we fixed the maximum hypocentral distance at 150 km. The left panels of figures 6 and 7 show the comparison of our GMPEs (represented as black lines) with FRI05 (grey dashed lines) and MAS07 (black dashed lines) models, for PGA and PGV, respectively. In those figures, the GMPEs have been plotted by assuming the central value of each magnitude class as the reference magnitude. In those figures, we compared our corrected GMPEs with respect to the FRI05 and MAS07 models with no site effect. When analysing the comparison results, it should be accounted that the MAS07 model assumes a local magnitude of 2.5 as the lower magnitude limit and then it has been extrapolated for the first magnitude class.

First of all, we note that the three models are characterized by a different attenuation with distance. In particular, concerning PGA, the differences in the trends depend on the distance range that is considered. In fact, the model retrieved in this study is characterized by a larger attenuation

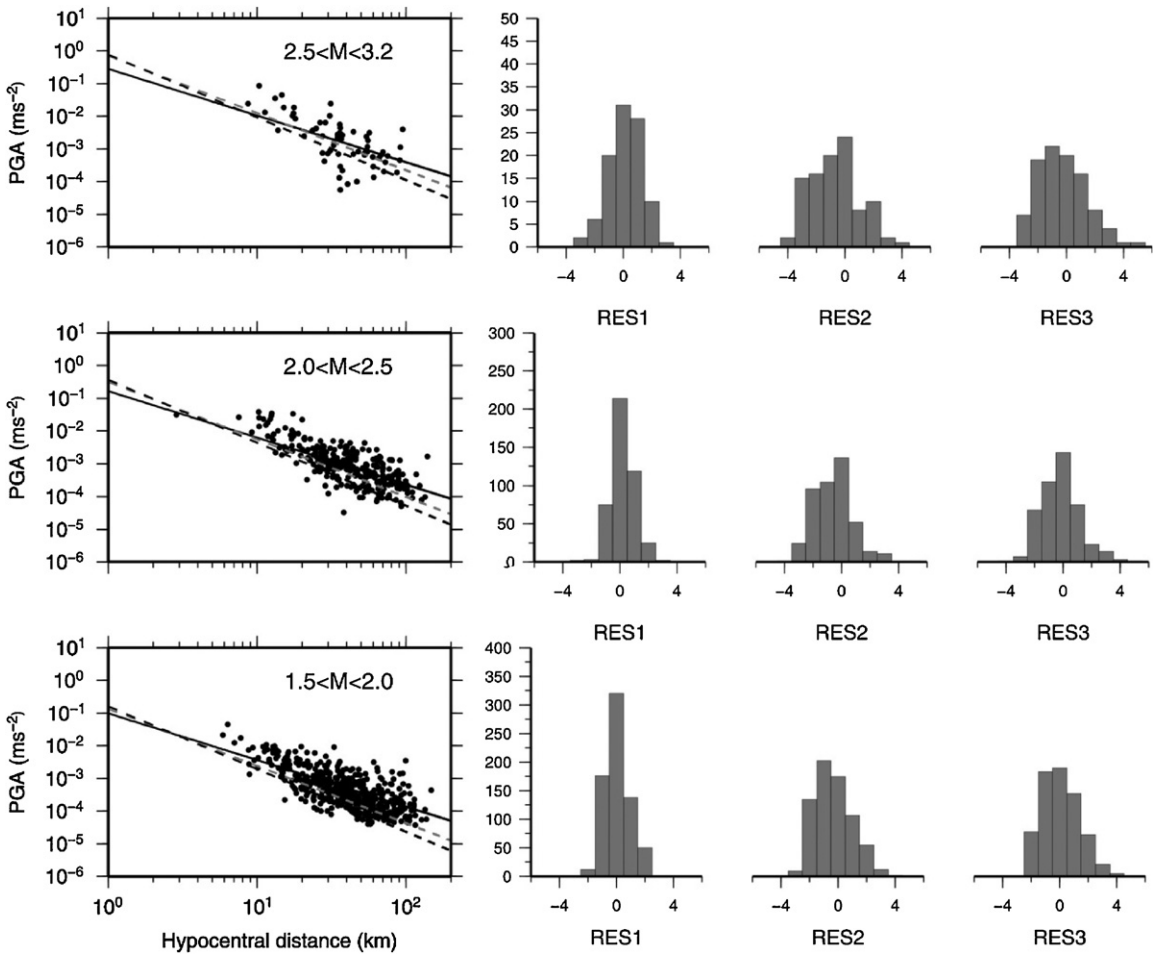

Figure 6. In the left panels, the observed PGA values (black dots), as a function of the hypocentral distance, are compared with respect to the GMPEs obtained in this study (black continuous lines), the MAS07 model (Massa *et al* 2007; black dashed lines), and the FRI05 model (Frisenda *et al* 2005; grey dashed lines). The comparison is performed dividing all available data into the three local-magnitude classes indicated in the plots. For the same classes, the right panels show the residuals, computed according to equation (5), with respect to our GMPEs (RES1), MAS07 model (RES2) and FRI05 model (RES3).

for distances less than 10 km while a lower attenuation is observed at larger distances. Those differences could be attributed both to a difference in tectonics of the region where data have been collected, and to the limited number of data at small distances. Moreover, due to the average depth of the earthquakes (about 14 km) analysed, the comparison for hypocentral distances less than 10 km may not be considered significant. When PGVs are considered, the differences are less marked and the three models are much more similar.

As an additional result, the right panels in figures 6 and 7 show the residuals distributions, defined according to equation (5), with respect to our GMPEs (RES1), to the MAS07 model (RES2) and to the FRI05 relationships (RES3). The differences between the three models also affect, of course, the residuals distributions. In particular, it should be noted that, for the magnitude classes containing larger number of data, the model retrieved in this paper provides zero-mean residuals distributions characterized by lower dispersion with respect to the other two models.

5. Conclusions

In this paper, we have retrieved ground-motion predictive equations (GMPEs) for low-magnitude earthquakes ($M_L < 3.2$) by using a dataset of 123 seismic events recorded at ISNet network, in the Campania–Lucania region in Southern Italy. The retrieved GMPEs, which allow for estimated peak ground acceleration (PGA) and peak ground velocity (PGV), will be specifically used both for ground-shaking map computation and for monitoring purposes.

The main conclusions of this work can be summarized as follows.

- The GMPEs obtained in this study represent a useful tool for ground-shaking map computation in the framework of a research project in collaboration with the Italian Department of Civil Protection and National Institute of Geophysics and Volcanology. They will be also used in future application related to hazard analyses for aftershocks. The range of validity corresponds to local magnitude values between 1.5 and 3.2 and hypocentral distances up to 100 km.

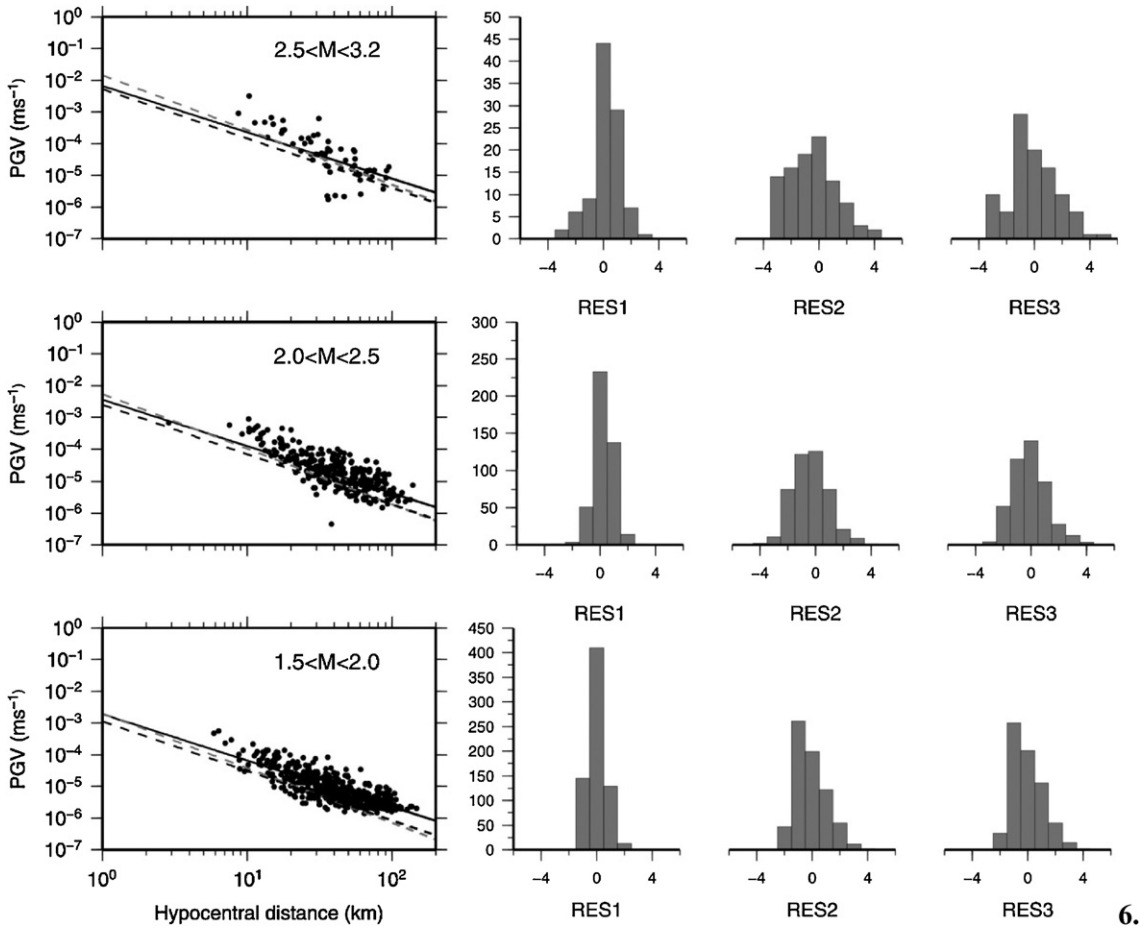

Figure 7. Same as figure 4 but for PGV.

- The dataset used in this study did allow us to implement a standard attenuation model. In fact, additional coefficients aimed at accounting for a quadratic magnitude dependence or a linear distance dependence were found to be statistically negligible. Moreover, the c coefficient in equation (6) has been found to be different from -1, indicating that, for the selected low-magnitude earthquakes, PGAs and PGVs are related to seismic phases different from direct body waves and that anelastic attenuation effects have to be studied.
- We have proposed a strategy based on the statistical Z-test, aimed at discriminating those stations of the ISNet network that are affected by some effect different from site effect accounted, at first order, by corrective coefficients based on the QVTM map. We have found that many receivers are characterized by such a station effect.
- The GMPEs retrieved in this study have been compared to FRI05 and MAS07 models which, fundamentally, have the same formulation. For the selected magnitude and distance ranges, our GMPEs show a better fit to observed data, for both PGA and PGV. Figures 6 and 7 enlighten the main differences between the three models. These differences could be attributed both to the inhomogeneity in the earthquake focal mechanism and to different attenuation properties of the tectonic areas where data, on which models are based, have been collected. Both are of relevance when low-magnitude earthquakes are considered. Similar results have been found by Atkinson and Morrison (2009) for small-to-moderate earthquakes in North America.
- As the dataset of earthquakes recorded at the ISNet network will increase, both in terms of earthquakes and in the magnitude range, in the future, starting from the model retrieved in this study, an updated version of the GMPEs for moderate earthquakes could be calibrated following the recipes of this paper.

Acknowledgments

This research has benefited from funding provided by the Italian Presidenza del Consiglio dei Ministri – Dipartimento della Protezione Civile (DPC) in the framework of the research project S3 (agreement 2007–2009 between DPC and INGV). Scientific papers funded by DPC do not represent its official opinion and policies. The authors wish to thank M Massa and two anonymous referees for their useful comments that improved the quality of the manuscript. The figures were prepared with Generic Mapping Tools (Wessel and Smith 1991).

Appendix. Ground-motion data

Table A1. Peak ground-motion values for some selected earthquakes. The QVTM class for each site is listed in table 4.

Earthquake yr-mo-day	Event latitude	Event longitude	Magnitude	Station code	Hypocentral distance (km)	PGA (m s^{-2})	PGV (m s^{-1})
2009-05-18	40.87	15.19	1.5	NSC3	6.5	5.3E-03	6.4E-05
				TEO3	6.6	1.0E-03	1.7E-05
				MNT3	16.0	6.8E-04	8.6E-06
				SNR3	14.5	1.0E-03	2.6E-05
				AND3	13.9	1.4E-04	3.8E-06
				COL3	23.0	6.1E-04	6.8E-06
				CMP3	25.5	5.2E-04	1.3E-05
				VDS3	24.1	2.4E-04	4.8E-06
				SCL3	32.8	2.2E-04	4.3E-06
				BEL3	40.9	8.3E-05	2.0E-06
				CGG3	45.4	1.1E-04	3.3E-06
				CLT3	18.3	2.7E-04	5.2E-06
				CSG3	23.4	5.9E-05	1.9E-06
				PST3	34.1	2.2E-04	4.8E-06
				RDM3	28.9	4.9E-05	1.9E-06
				RSF3	11.2	2.2E-04	3.5E-06
				SRN3	47.7	8.4E-05	1.9E-06
				STN3	53.6	4.7E-05	2.9E-06
2009-02-26	40.81	15.34	1.6	CSG3	11.5	2.0E-03	3.7E-05
				VDS3	11.4	6.0E-03	1.2E-04
				COL3	14.2	4.9E-03	6.5E-05
				SCL3	19.5	2.4E-03	4.4E-05
				AND3	14.6	3.9E-04	7.9E-06
				SNR3	15.6	1.2E-03	2.6E-05
				BEL3	27.3	1.8E-04	7.8E-06
				CGG3	33.4	6.3E-04	1.2E-05
				CMP3	28.3	1.0E-03	2.0E-05
				MNT3	28.8	6.5E-04	9.4E-06
				SRN3	37.2	3.1E-04	7.0E-06
				CLT3	13.0	1.7E-03	4.3E-05
				STN3	40.6	8.2E-05	2.5E-06
				AVG3	33.0	1.1E-04	3.3E-06
				PGN3	46.6	1.0E-04	2.2E-06
				RDM3	18.8	5.7E-04	1.9E-05
				RSF3	22.9	2.9E-04	4.4E-06
				TEO3	9.3	7.8E-04	1.3E-05
				VDP3	30.0	1.6E-03	6.8E-06
2008-10-06	40.86	15.14	1.7	RSF3	12.2	4.0E-03	3.7E-05
				AND3	18.4	6.3E-04	1.4E-05
				CLT3	23.1	7.1E-04	2.4E-05
				COL3	25.7	7.5E-04	1.4E-05
				CMP3	24.2	1.2E-03	2.3E-05
				CGG3	48.3	2.1E-04	5.0E-06
				AVG3	50.8	3.5E-04	4.1E-06
				BEL3	45.3	6.0E-05	2.2E-06
				CSG3	28.1	1.5E-04	3.5E-06
				MNT3	11.8	2.7E-03	4.4E-05
				PGN3	64.3	5.3E-05	2.0E-06
				PST3	34.9	2.9E-04	7.2E-06
				RDM3	33.7	1.7E-04	6.7E-06
				SCL3	36.8	2.7E-04	5.3E-06
				SNR3	15.3	2.5E-03	6.0E-05
				SRN3	50.0	1.1E-04	2.2E-06
				TEO3	11.3	1.8E-03	3.8E-05
				VDP3	46.6	2.1E-03	6.3E-06
				VDS3	28.1	3.0E-04	8.3E-06
2008-10-20	41.05	14.75	1.8	MNT3	32.3	3.1E-04	7.8E-06
				NSC3	38.9	1.1E-04	5.2E-06
				CMP3	52.2	1.9E-04	6.7E-06
				SNR3	51.2	1.6E-04	6.0E-06
				VDS3	66.6	7.4E-05	3.0E-06
				AND3	51.2	9.4E-05	2.7E-0

Table A1. (Continued.)

Earthquake yr-mo-day	Event latitude	Event longitude	Magnitude	Station code	Hypocentral distance (km)	PGA (m s^{-2})	PGV (m s^{-1})
				AVG3	88.1	1.4E-054	2.0E-06
				BEL3	83.5	9.9E-05	1.8E-06
				CGG3	86.1	4.5E-05	2.4E-06
				CLT3	57.7	3.1E-04	3.6E-06
				COL3	63.4	5.9E-05	2.3E-06
				CSG3	65.5	4.6E-05	2.8E-06
				PGN3	102.9	5.4E-05	1.9E-06
				PST3	68.3	5.3E-05	3.0E-06
				RDM3	69.1	1.4E-04	1.8E-06
				RSF3	37.6	7.3E-05	3.2E-06
				SCL3	75.3	2.1E-04	1.8E-06
				SRN3	86.4	3.5E-03	4.0E-06
				TEO3	49.1	1.3E-03	2.4E-06
2009-05-15	40.66	15.40	1.9	COL3	10.1	6.6E-03	9.3E-05
				SCL3	13.1	4.2E-03	9.9E-05
				VDS3	12.1	3.5E-03	6.6E-05
				CGG3	18.9	2.5E-03	6.0E-05
				SNR3	20.6	1.1E-03	2.4E-05
				BEL3	22.5	5.3E-04	3.0E-05
				CMP3	27.9	3.2E-03	8.2E-05
				STN3	27.3	3.7E-04	8.9E-06
				CLT3	27.8	5.6E-04	1.7E-05
				NSC3	31.8	6.5E-04	1.1E-05
				RDM3	27.5	2.6E-04	9.9E-06
				MNT3	38.9	7.1E-04	8.6E-06
				AND3	31.2	4.1E-04	1.1E-05
				AVG3	30.8	4.2E-04	5.2E-06
				CSG3	19.8	4.6E-04	1.0E-05
				PGN3	36.1	1.6E-04	4.0E-06
				PST3	19.0	3.0E-03	5.5E-05
				RSF3	39.1	4.3E-03	1.1E-05
				SRN3	21.8	8.8E-04	2.2E-05
				TEO3	24.4	1.3E-03	9.3E-06
				VDP3	18.0	1.6E-03	3.1E-05
2009-05-18	40.74	15.33	2.0	COL3	6.5	4.4E-02	5.7E-04
				VDS3	8.6	9.3E-03	2.1E-04
				CSG3	14.6	8.5E-04	2.4E-05
				SNR3	12.3	4.7E-03	1.2E-04
				TEO3	13.8	1.2E-03	4.7E-05
				NSC3	21.8	6.4E-04	1.4E-05
				SCL3	16.1	2.7E-03	5.2E-05
				AND3	21.7	2.3E-04	1.0E-05
				CLT3	19.7	6.6E-04	2.8E-05
				CMP3	23.5	2.5E-03	7.4E-05
				BEL3	25.9	2.4E-04	1.6E-05
				CGG3	27.1	6.5E-04	2.6E-05
				MNT3	29.8	8.5E-04	1.3E-05
				RDM3	23.2	4.2E-04	1.6E-05
				STN3	35.5	1.2E-04	5.2E-06
				AVG3	33.3	9.4E-05	4.6E-06
				PGN3	43.2	7.8E-05	3.0E-06
				PST3	21.2	1.1E-03	2.5E-05
				RSF3	28.7	2.1E-04	4.3E-06
				SRN3	29.9	3.6E-04	1.2E-05
				VDP3	25.1	1.4E-03	1.3E-05
2008-06-25	41.31	15.88	2.1	AND3	63.5	1.8E-04	5.3E-06
				AVG3	63.4	1.2E-04	3.0E-06
				BEL3	70.2	1.8E-04	8.2E-06
				CGG3	91.2	1.5E-04	3.3E-06
				CLT3	61.5	5.5E-04	1.1E-05
				CMP3	99.9	1.3E-04	3.1E-06
				COL3	84.0	1.5E-04	4.1E-06
				CSG3	66.0	6.0E-05	2.0E-06

Table A1. (Continued.)

Earthquake yr-mo-day	Event latitude	Event longitude	Magnitude	Station code	Hypocentral distance (km)	PGA (m s^{-2})	PGV (m s^{-1})
				LIO3	75.4	2.0E-04	2.1E-06
				MNT3	90.8	1.5E-04	2.4E-06
				NSC3	82.6	1.3E-04	2.2E-06
				PGN3	83.1	1.5E-04	2.5E-06
				PST3	99.6	1.2E-04	2.9E-06
				RDM3	57.5	1.7E-04	3.6E-06
				RSF3	71.3	3.7E-04	4.3E-06
				SCL3	75.9	2.8E-02	5.5E-05
				SNR3	86.8	1.3E-04	3.5E-06
				SRN3	98.9	7.6E-05	3.4E-06
				STN3	89.5	1.7E-04	2.8E-06
				TEO3	74.1	6.8E-04	2.3E-06
				VDP3	83.3	7.1E-04	5.2E-06
2009-09-01	40.82	15.29	2.2	TEO3	15.2	4.2E-03	6.3E-05
				AND3	19.8	7.5E-04	1.7E-05
				CLT3	20.2	1.2E-03	3.7E-05
				COL3	20.8	5.4E-03	5.3E-05
				CSG3	20.9	5.6E-04	1.1E-05
				LIO3	19.5	4.2E-04	8.8E-06
				NSC3	20.5	1.8E-03	3.7E-05
				RSF3	24.0	8.0E-04	1.0E-05
				SNR3	19.0	2.7E-03	7.7E-05
				VDS3	20.6	1.3E-03	2.5E-05
				MNT3	27.9	1.5E-03	1.8E-05
				SCL3	27.4	1.3E-03	1.9E-05
				CMP3	29.2	2.0E-03	2.9E-05
				RDM3	26.4	4.4E-04	3.1E-05
				AVG3	40.1	2.1E-04	3.3E-06
				BEL3	34.7	1.9E-04	1.2E-05
				CGG3	39.1	9.7E-04	1.7E-05
				STN3	46.5	1.4E-04	3.5E-06
				PGN3	52.8	8.0E-05	2.7E-06
				PST3	32.1	6.8E-04	1.1E-05
				SRN3	42.0	2.0E-04	5.9E-06
2009-08-30	40.62	15.44	2.3	CGG3	11.5	5.2E-03	1.5E-04
				SCL3	10.8	1.8E-02	5.2E-04
				COL3	12.0	3.0E-03	8.0E-05
				STN3	20.7	1.2E-03	2.1E-05
				VDS3	13.8	2.1E-03	8.9E-05
				BEL3	20.0	9.7E-04	6.3E-05
				CSG3	22.3	3.2E-04	1.9E-05
				SNR3	24.5	9.1E-04	2.8E-05
				AVG3	29.0	3.3E-04	1.2E-05
				CMP3	30.4	1.2E-03	2.5E-05
				NSC3	36.7	1.2E-03	8.2E-06
				RDM3	29.7	2.5E-04	1.5E-05
				MNT3	43.6	8.4E-04	8.7E-06
				AND3	35.7	8.8E-04	1.2E-05
				CLT3	31.7	6.2E-04	9.1E-06
				LIO3	37.7	1.8E-04	4.1E-06
				PGN3	30.8	2.1E-04	1.1E-05
				PST3	17.8	1.3E-03	3.1E-05
				SRN3	15.1	1.8E-03	6.1E-05
				TEO3	29.1	9.7E-04	2.5E-06
				VDP3	11.7	2.6E-03	1.0E-04
2008-11-08	40.18	16.03	2.4	AND3	102.1	1.1E-04	2.9E-06
				AVG3	69.8	1.7E-04	2.0E-06
				BEL3	68.3	8.5E-05	3.3E-06
				CGG3	59.1	1.1E-03	1.1E-05
				CLT3	96.2	5.7E-05	1.9E-06
				CMP3	96.0	4.6E-04	4.5E-06
				COL3	81.9	2.3E-04	3.9E-06
				CSG3	85.7	5.0E-05	1.9E-06

Table A1. (Continued.)

Earthquake yr-mo-day	Event latitude	Event longitude	Magnitude	Station code	Hypocentral distance (km)	PGA (m s^{-2})	PGV (m s^{-1})
				MNT3	113.2	9.7E-05	2.6E-06
				NSC3	106.7	2.1E-04	2.3E-06
				PGN3	48.2	4.0E-04	5.4E-06
				PST3	79.1	2.2E-04	5.2E-06
				RDM3	87.9	1.0E-04	2.0E-06
				RSF3	113.1	2.2E-03	1.4E-05
				SCL3	72.3	1.3E-03	1.7E-05
				SNR3	94.0	9.0E-05	2.4E-06
				SRN3	59.5	2.5E-04	6.6E-06
				TEO3	98.3	1.0E-03	4.9E-06
				VDP3	61.3	5.4E-04	5.4E-06
				VDS3	80.7	2.6E-04	3.8E-06
2008-11-14	40.62	15.77	2.5	AVG3	22.1	2.6E-03	6.1E-05
				BEL3	21.5	2.9E-03	1.4E-04
				SCL3	27.7	2.6E-03	6.9E-05
				VDP3	22.7	2.0E-03	5.0E-05
				CGG3	27.4	4.9E-03	1.0E-04
				VDS3	35.1	1.5E-03	6.2E-05
				CMP3	60.0	1.3E-03	3.8E-05
				COL3	40.5	2.8E-03	6.5E-05
				CSG3	36.8	6.0E-04	2.9E-05
				NSC3	61.6	6.8E-04	1.4E-05
				PGN3	16.8	7.3E-03	2.1E-04
				RDM3	37.4	9.7E-04	2.1E-05
				RSF3	64.3	4.1E-04	7.6E-06
				SRN3	34.0	1.4E-03	3.5E-05
				TEO3	51.3	1.6E-03	8.9E-06
				CLT3	46.1	1.7E-03	2.7E-05
				PST3	47.4	9.0E-04	2.4E-05
				AND3	52.2	6.6E-04	1.1E-05
				SNR3	52.3	1.7E-03	4.2E-05
				MNT3	69.9	6.1E-04	1.3E-05
2009-04-16	40.22	15.61	2.6	AND3	82.9	1.3E-04	2.6E-06
				AVG3	61.9	1.4E-04	2.6E-06
				BEL3	56.0	1.5E-04	4.7E-06
				CGG3	37.9	2.6E-03	5.9E-05
				CLT3	78.5	1.3E-04	3.5E-06
				CMP3	66.3	6.0E-04	1.5E-05
				COL3	57.9	5.7E-04	1.1E-05
				MNT3	85.9	3.9E-03	1.8E-05
				NSC3	81.5	1.9 E-04	3.8E-06
				PGN3	43.5	7.0E-04	1.7E-05
				PST3	49.9	1.8E-03	3.3E-05
				RDM3	73.8	9.7E-05	2.7E-06
				RSF3	91.0	1.8E-04	2.2E-06
				SCL3	54.4	7.8E-04	1.7E-05
				SNR3	68.0	3.9E-04	9.0E-06
				SRN3	33.7	2.3E-03	3.4E-05
				STN3	36.1	6.9E-04	2.1E-05
				TEO3	76.0	1.3E-03	5.2E-06
				VDP3	44.1	5.2E-04	9.1E-06
				VDS3	60.7	2.9E-04	7.2E-06
2009-02-28	40.49	15.55	2.7	CGG3	8.7	2.4E-02	8.9E-04
				SRN3	9.4	1.3E-02	4.6E-04
				STN3	11.7	3.7E-03	1.6E-04
				SCL3	24.1	3.6E-03	5.8E-05
				BEL3	27.2	9.5E-04	6.1E-05
				COL3	29.4	1.3E-03	5.0E-05
				VDS3	30.6	8.7E-04	4.5E-05
				AVG3	34.6	2.9E-04	1.9E-05
				SNR3	41.1	8.2E-04	3.0E-05
				CMP3	43.8	1.2E-03	5.7E-05
				RDM3	43.6	2.6E-04	1.5E-05

Table A1. (Continued.)

Earthquake yr-mo-day	Event latitude	Event longitude	Magnitude	Station code	Hypocentral distance (km)	PGA (m s^{-2})	PGV (m s^{-1})
				MNT3	60.1	2.0E-04	8.4E-06
				AND3	52.7	2.9E-04	9.6E-06
				CSG3	38.0	2.2E-04	1.3E-05
				PGN3	23.9	7.2E-04	4.7E-05
				TEO3	46.7	2.6E-03	2.0E-05
				VDP3	14.6	2.1E-03	1.0E-04
2008-11-08	40.59	15.56	2.8	VDP3	8.4	2.5E-01	4.2E-03
				CGG3	10.0	8.5E-02	3.2E-03
				SCL3	15.0	1.8E-02	4.1E-04
				SRN3	16.3	1.8E-02	5.5E-04
				BEL3	17.6	4.7E-03	2.7E-04
				VDS3	22.0	3.7E-03	1.5E-04
				AVG3	25.2	7.5E-04	4.6E-05
				COL3	23.7	6.4E-03	1.8E-04
				PST3	28.0	4.5E-03	1.2E-04
				CSG3	28.1	4.3E-04	3.1E-05
				SNR3	36.0	3.4E-03	6.8E-05
				CLT3	38.3	5.4E-04	2.2E-05
				CMP3	41.8	2.4E-03	6.3E-05
				NSC3	47.5	3.1E-03	1.2E-05
				RDM3	33.1	7.8E-04	3.2E-05
				AND3	43.3	2.4E-04	1.7E-05
				MNT3	54.8	6.4E-04	1.4E-05
				PGN3	21.6	2.5E-03	1.1E-04
				RSF3	53.5	3.2E-04	1.0E-05
				TEO3	38.8	5.9E-04	2.7E-05
2008-10-11	40.73	15.35	3.2	AND3	22.6	3.3E-04	9.0E-06
				AVG3	32.3	1.8E-04	3.0E-06
				BEL3	24.8	1.6E-04	5.4E-06
				CGG3	25.7	1.3E-04	5.9E-06
				CLT3	20.2	2.4E-04	9.5E-06
				CMP3	24.0	2.4E-04	1.1E-05
				COL3	5.5	3.2E-04	6.4E-06
				CSG3	14.4	1.4E-04	5.4E-06
				MNT3	31.0	7.0E-04	4.7E-06
				PGN3	41.9	4.4E-03	4.8E-06
				PST3	20.7	2.1E-04	5.7E-06
				RDM3	23.1	1.1E-04	7.1E-06
				RSF3	29.9	7.0E-04	7.9E-06
				SCL3	14.7	1.2E-04	5.1E-06
				SNR3	13.2	1.8E-04	7.4E-06
				SRN3	28.7	7.2E-05	5.6E-06
				TEO3	14.9	1.9E-03	8.0E-06
				VDP3	23.7	1.0E-03	7.6E-06
				VDS3	7.6	1.1E-03	9.3E-06

References

Abrahamson N A and Silva W J 1997 Empirical response spectral attenuation relations for shallow crustal earthquakes *Seismol. Res. Lett.* **68** 94–127

Akkar S and Bommer J J 2007 Empirical prediction equations for peak ground velocity derived from strong-motion records from Europe and the Middle East *Bull. Seismol. Soc. Am.* **97** 511–30

Allen R M and Kanamori H 2003 The potential for earthquake early warning in Southern California *Science* **300** 786–9

Atkinson G M 2006 Single-station sigma *Bull. Seismol. Soc. Am.* **96** 446–55

Atkinson G M and Morrison M 2009 Observations on regional variability in ground motion amplitudes from small-to-moderate earthquakes in North America *Bull. Seismol. Soc. Am.* **89** 2393–409

Bernard P and Zollo A 1989 The Irpinia (Italy) 1980 earthquake: detailed analysis of a complex normal fault *J. Geophys. Res.* **94** 1631–48

Beyer K and Bommer J J 2006 Relationships between median values and aleatory variabilities for different definitions of the horizontal component of motion *Bull. Seismol. Soc. Am.* **94** 1512–22

Bobbio A, Vassallo M and Festa G 2009 A local magnitude scale for Southern Italy *Bull. Seismol. Soc. Am.* **99** 2461–70

Boore D M and Atkinson G M 2008 Ground motion prediction equations for the mean horizontal component of PGA, PGV and 5%-damped PSA at spectral periods between 0.01 s and 10.0 s *Earthq. Spectra* **24** 99–138

Borcherdt R D 1970 Effects of local geology on ground motion near San Francisco Bay *Bull. Seismol. Soc. Am.* **60** 29–61

Borcherdt R D 1994 Estimates of site-dependent response spectra for design (methodology and justification) *Earthq. Spectra* **10** 617–54

Boschi E, Ferrari G, Gasperini P, Guidoboni E, Smriglio G and Valensise G 1995 *Catalogo dei Forti Terremoti in Italia dal 461 A.C. al 1980* (Bologna: ING-SGA) p 973

Bragato P L and Slejko D 2005 Empirical ground-motion attenuation relations for the Eastern Alps in the magnitude range 2.5–6.3 *Bull. Seismol. Soc. Am.* **95** 252–76

Cantore L 2008 Determination of site amplification in the Campania–Lucania region (Southern Italy) by comparison of different site-response estimation techniques *PhD Thesis* University 'Federico II', Naples, Italy

Cantore L, Convertito V and Zollo A 2010 Development of a site conditions map for the Campania–Lucania region (Southern Apennines, Italy) *Ann. Geophys.* **53** at press doi:10.4401/ag-4648

CEN, European Committee for Standardization 2004 *Eurocode 8: Design of Structures for Earthquake Resistance—Part 1. General Rules, Seismic Actions and Rules for Buildings* (Brussels: Comité Européen de Normalisation)

Convertito V, De Matteis R, Cantore L, Zollo A, Iannaccone G and Caccavale M 2010 Rapid estimation of ground-shaking maps for seismic emergency management in the Campania Region of Southern Italy *Nat. Hazards* **52** 97–115

Douglas J 2007 On the regional dependence of earthquake response spectra *ISET J. Earthq. Technol.* **44** 71–99

Emolo A and Zollo A 2005 Kinematic source parameters for the 1989 Loma Prieta earthquake from the nonlinear inversion of accelerograms *Bull. Seismol. Soc. Am.* **95** 981–94

Frisenda M, Massa M, Spallarossa D, Ferretti G and Eva C 2005 Attenuation relationship for low magnitude earthquakes using standard seismometric records *J. Earthq. Eng.* **9** 23–40

Iannaccone G *et al* 2010 A prototype system for earthquake early-warning and alert management in Southern Italy *Bull. Earthq. Eng.* **8** 1105–29

Joyner W B and Fumal T E 1985 Predictive mapping of earthquake ground motion *Evaluating Earthquake Hazard in the Los Angeles Region—An Earth-Science Perspective US Geol. Survey Prof. Pap. 1360* ed J I Ziony pp 203–20

Massa M, Marzorati S, D'Alema E, Di Giacomo D and Augliera P 2007 Site classification assessment for estimating empirical attenuation relationships for Central-Northern Italy earthquakes *J. Earthq. Eng.* **11** 943–67

Michelini A, Faenza L, Lauciani V and Malagnini 2008 Shakemap implementation in Italy *Seismol. Res. Lett.* **79** 688–97

Park S and Elrick S 1998 Predictions of shear wave velocities in Southern California using surface geology *Bull. Seismol. Soc. Am.* **88** 677–85

Reiter L 1990 *Earthquake Hazard Analysis* (New York: Columbia University Press) p 254

Trifunac M D and Brady A G 1975 A study on the duration of strong earthquake ground motion *Bull. Seismol. Soc. Am.* **65** 581–626

Wald D J, Quitoriano V, Heaton T H, Kanamori H, Scrivner C W and Worden C B 1999 TriNet shakemaps: rapid generation of instrumental ground motion and intensity maps for earthquakes in Southern California *Earthq. Spectra* **15** 537–55

Weber E *et al* 2007 An advanced seismic network in Southern Apennines (Italy) for seismicity investigations and experimentation with earthquake early warning *Seismol. Res. Lett.* **78** 622–34

Wessel P and Smith W H F 1991 Free software helps map and display data *EOS Trans. AGU* **72** 445–6